Self-Adhesion of Polyethylene in the Melt. 1. Heterogeneous Copolymers

N. Z. Qureshi,[†] E. V. Stepanov,[†] G. Capaccio,[‡] A. Hiltner,*[,†] and E. Baer[†]

Department of Macromolecular Science and Center for Applied Polymer Research, Case Western Reserve University, Cleveland, Ohio 44106-7202, and BP Amoco Chemicals, Applied Technology, Grangemouth, FK3 9XH, U.K.

Received March 31, 2000; Revised Manuscript Received November 3, 2000

ABSTRACT: Development of self-adhesion above the melting temperature was studied in a group of linear low-density polyethylenes. An experimental procedure for consecutively sealing and peeling a polymeric film at the same temperature, above the melting point, was developed. This made it possible to measure melt adhesion over a wide range of temperatures, seal times, and peel rates. Taking advantage of the new experimental technique, the molecular mechanisms and kinetics of self-adhesion in heterogeneous ethylene copolymers with broad molecular weight distribution were investigated. It was found that the peel strength increased with the contact time in accordance with the conventional $t^{1/2}$ dependence until saturation at the maximum strength. The time to achieve maximum strength was significantly shorter for the copolymer with more homogeneous copolymer composition; however, the maximum strength was the same for all the materials at each test temperature. The saturation time in all cases was 2 orders of magnitude longer than the time for complete interdigitation of the surface chains. This was ascribed to the presence of a surface layer of about 100 nm that needed to resolve after sealing the surfaces before the maximum adhesive strength could develop. The layer was thought to originate from surface segregation of the lower molecular weight, higher branch content fraction of the material.

Introduction

Fundamental understanding of molecular mechanisms responsible for macromolecular adhesion is currently a lively topic.[1−7] Activity in this area is motivated, on one hand, by recent advances in catalyst technology that make available new families of polymeric materials and new levels of control on chemical composition and molecular architecture.[2,8−10] On the other hand, significant advances in the theory of polymer dynamics[11,12] make possible deeper understanding of the relationship between the polymer structure and adhesion from the viewpoint of basic molecular processes.

Self-adhesion in the melt is a specific type of adhesion. Developed through mutual diffusion and interdigitation of interfacial chains, self-adhesion is directly related to the molecular structure of the material. The strength of the self-adhesion bond is of practical importance to heat seal and hot tack performance of polymeric films. The relationship to heat seal is not apparent from the common practice of measuring heat seal by a fracture test at ambient temperature.[1−3] The hot tack test[13−15] is closer to a measure of self-adhesion in the melt. Typical results obtained with a commercial hot tack tester in Figure 1 compare the performance of four polyethylene copolymers of approximately the same density. In this test, the homogeneous metallocene copolymer had the highest hot tack strength, about twice the value for the heterogeneous Ziegler−Natta copolymers. Some variation was also found among the heterogeneous copolymers. Recognizing that even measurements of hot tack with a nonisothermal commercial tester include contributions from crystallization, some authors have tried to interpret hot tack data in relation to crystallization kinetics.[16] However, the energy consumed upon fracturing a semicrystalline polymer is mainly determined by yielding and morphological reorganization of the crystal phase,[17] and the contribution of melt adhesion cannot be readily extracted. Thus, a realistic test of melt adhesion should be performed in the melt at the same temperature used for heat sealing.

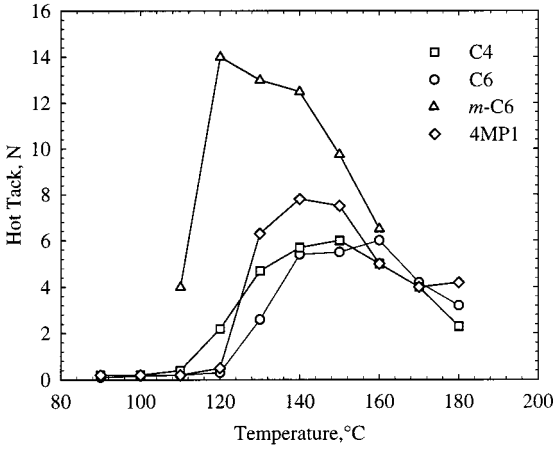

Figure 1. Conventional hot tack test data for polyethylene copolymers. Data provided by BP Amoco Chemicals.

In the present study, a technique for consecutively sealing and peeling film specimens at the same temperature, above the melting point, was developed. This made possible the first direct measurements of melt adhesion in a wide range of temperatures, sealing times, and peeling rates. Taking advantage of the new experimental technique, the molecular mechanisms and kinetics of adhesion in short-chain branched linear polyethylene with broad molecular weight distribution were explored. The study was performed specifically on the three heterogeneous copolymer films used to obtain the hot tack data in Figure 1.

With these materials, we hoped to elucidate the role of certain features of the molecular composition such as polydispersity in molecular weight and heterogeneity

[†] Case Western Reserve University.
[‡] BP Amoco Chemicals.
* Corresponding author.

10.1021/ma000583x CCC: $20.00
Published on Web 01/30/2001

Table 1. Copolymer Characterization

polymer designation	comonomer	density (g/cm^3)	avg branch concn (per 1000C)	M_w (g/mol)	M_w/M_n	ΔH (J/g)	T_m (°C)
C4	butene	0.9193	~20	118 100	4.0	134	123
C6	hexene	0.9169	~20	118 500	3.7	128	125
4MP1	4-methyl-pentene-1	0.9167	~20	111 000	3.6	136	126

in comonomer content that are intrinsic to most commercial polyethylenes.[18] It is known from studies of adhesion in monodisperse species that both the dynamics of surface chain interdigitation and the maximum adhesion (cohesive strength) depend strongly on molecular weight.[1,2] A recent investigation of interdiffusion kinetics in microlayers of highly polydisperse polyethylenes revealed the time scale for consecutive participation of different molecular weight fractions in interfacial mass transfer.[19,20] However, the role of different fractions in developing adhesive strength in a real material is not well understood.

Structural heterogeneity of ethylene copolymers takes the form of excessive concentration of short chain branches on highly mobile chains of low molecular weight.[18] A previous investigation indicated that branching decreases the interdiffusion rate.[19] Nevertheless, the potential effect of short-chain branching on chain reptation dynamics has been largely neglected, despite the common use of hydrogenated polybutadienes in experimental studies of adhesion and interdiffusion.[21−23] Other effects arising from differences in interaction between chains with high and low branch content are expected. These differences are known to cause phase separation of monodisperse fractions extracted from a typical heterogeneous polyethylene.[24,25] The present work explores the effects of both polydispersity and molecular heterogeneity on self-adhesion of polyethylenes in the melt by testing a selected series of polyethylene copolymers of well-characterized molecular composition.

Experimental Section

Materials. Three linear low-density polyethylenes described in Table 1 were provided by BP Amoco Chemicals as pellets and as blown film 50 μm thick. The comonomers were butene (C4), 4-methylpentene-1 (4MP1), and hexene (C6). The copolymers had similar average short-chain branch content and similar molecular weight as provided by the manufactuarer.

The copolymers were produced using a conventional Ziegler−Natta catalyst and were characterized by nonuniform comonomer placement. Temperature rising elution fractionation[26] (TREF) curves in Figure 2 revealed two peaks in the short chain branch distribution: a large peak containing fractions with higher branch concentrations and a smaller peak consisting of fractions with lower branch concentrations. The main peak was much larger for the C4 copolymer than for the 4MP1 and C6 copolymers. The second peak, which corresponded to chains with longer methylene sequences, was prominent in the curves of the 4MP1 and C6 copolymers but was much smaller and appeared almost as a shoulder in the curve of the C4 copolymer. Furthermore, the tail in the distribution extended to longer methylene sequence lengths for the 4MP1 and C6 copolymers than for the C4 copolymer. The TREF curves suggested that the C4 copolymer was more homogeneous in its branch distribution than the C6 and 4MP1 copolymers.

The densities of the materials were measured in a 2-propanol−distilled water density gradient column calibrated with glass floats. The melting temperature and heat of melting were obtained on blown films with the Rheometrics DSC using a heating rate of 10 °C min^{-1}.

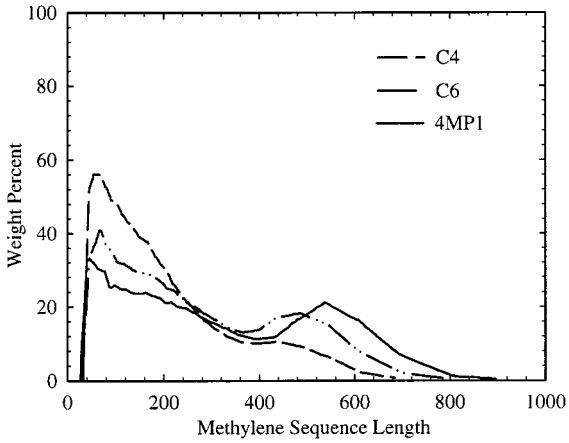

Figure 2. TREF curves for heterogeneous polyethylene copolymers. Data provided by BP Amoco Chemicals.

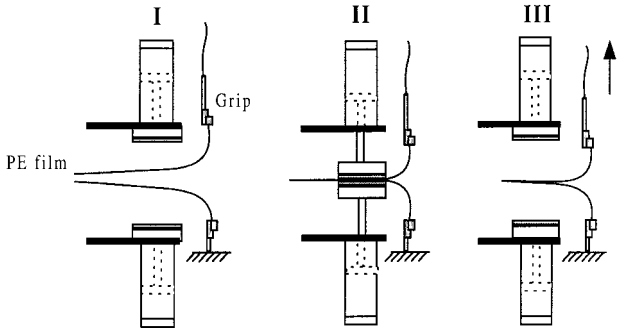

Figure 3. Schematic of the experimental setup for isothermal melt adhesion measurements.

Methods. The apparatus for isothermal peel testing consisted of a sealing device and a control unit. The sealing device contained two pneumatic cylinders that were mounted on a stage in the orientation shown in Figure 3 and connected to the control unit with high-temperature Teflon tubing. The apparatus was contained in the environmental chamber of an Instron testing machine. The control unit consisted of a main control valve, a thumb-controlled valve to activate the cylinders, and a pneumatic timer (model KLH-10, MEAD USA, Chicago, IL) that produced a minimum seal time of 0.5 s.

To construct the specimen, the outer surface of a 2.5 cm × 15 cm strip of polyethylene blown film was attached to a high-temperature adhesive tape (TESA 4108, Biersdorf AG Hamburg, Germany); the nonadhesive side of the tape was backed with a double-sided adhesive film (Scotch Brand 9485PC, 3M, St. Paul, MN) and adhered to Mylar. Two films with this construction were joined at one end with a staple so that the inner surfaces of the polyethylene film were facing. The specimen was loaded into the environmental chamber between the two cylinders, and the free ends were connected to the Instron grips. Sufficient tension was applied to the ends of the specimen to keep the films from coming in contact as they were brought to temperature. The specimens were allowed to equilibrate at the test temperature for 10 min before the thumb-controlled valve was activated to allow nitrogen to flow into the cylinders via the pneumatic timer to apply the seal. When the seal time expired, the cylinders retracted and the Instron was activated (Figure 3). The force was recorded as the sealed surfaces were peeled apart. The adhesive strength was calculated as $2P/w$ where P is the measured peel force

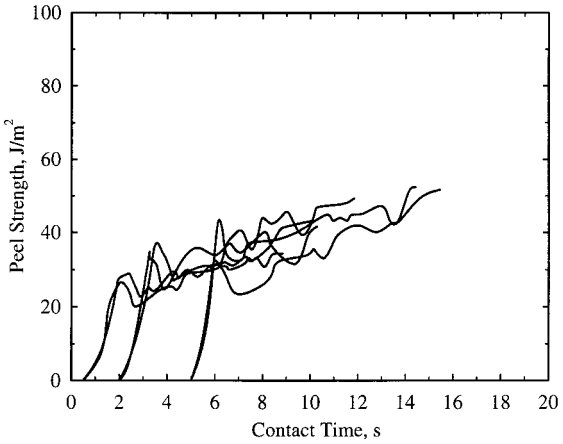

Figure 4. Peel curves of 4MP1 copolymer obtained at 135 °C with a peel rate of 500 mm min^{-1} for sealing times of 0.5, 2, and 5 s showing overlap in terms of the total contact time.

and w is the specimen width. Additional experiments with two layers of Mylar backing on the specimen produced no change in the measured peel force, indicating there was no significant contribution from plastic deformation of the peel arms to the measured peel force. In addition, it was found that varying the seal pressure from 0.20 to 0.70 MPa did not affect the peel force. In subsequent experiments, the seal pressure was 0.35 MPa. The seal time was varied from 0.5 to 25 s, and peel rates of 50 and 500 mm min^{-1} were used. At the melting temperature T_m, defined as the maximum in the DSC melting thermogram (Table 1), no adhesion was measured: the specimen fell apart upon peeling. The lowest temperature used in melt adhesion measurements was $T_m + 4$ °C, which corresponded to 127 °C for the C4 copolymer and 130 °C for the C6 and 4MP1 copolymers.

Results and Discussion

Melt Peel Curves. Isothermal melt adhesion data are shown in Figure 4 for the 4MP1 copolymer at 135 °C and seal times of 1, 2, and 5 s. Initially the peel force increased sharply until a crack initiated. This example was typical in showing a continuous increase in the peel force during propagation of the peel crack, unlike conventional peel curves where the crack propagates steadily after initiation. When the peel strength was plotted as a function of total contact time, i.e., the sum of the seal time and the peel time, the peel curves for different seal times overlapped.

Development of adhesion upon sealing two identical polymeric materials in the melt is usually ascribed to surface chain interdiffusion.[1−3] The overlap of the time dependence of the peel force after sealing for different times, taken together with the absence of a dependence on the seal pressure, indicated that bringing the surfaces into contact was enough to initiate interdiffusion over the contact area. Only the contact time was important for adhesion at a given temperature. During that time, chain interdiffusion continued in the unpeeled part of the specimen so that the crack propagated through an interface of gradually increasing adhesive strength. Thus, the time function of the peal force in the isothermal test above the melting temperature was indicative of the intrinsic molecular mechanisms of interdiffusion.

Examples for C4 and 4MP1 copolymers in Figures 5 and 6 illustrate the peel curves that were encountered. The C6 copolymer exhibited the same behavior as the 4MP1 copolymer at all experimental conditions tested. The experimental time dependence of the peel force was

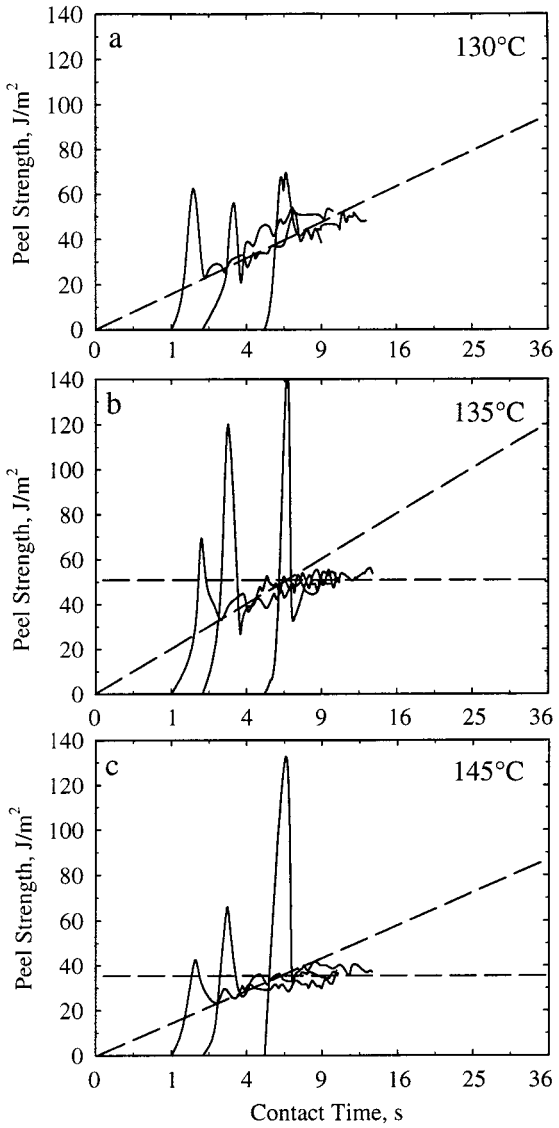

Figure 5. Peel curves of C4 copolymer at different melt temperatures obtained with a peel rate of 500 mm min^{-1} for sealing times of 1, 2, and 5 s plotted as a function of total contact time t. The time axis is linear with $t^{1/2}$.

obtained by finding the best power fit of the data with zero intercept. All the peel curves clearly showed a $t^{1/2}$ dependence at short contact times. The data suggested that at longer times the peel force reached a maximum and time-independent value (t^0 dependence). The times to saturation were significantly different for the C4 and 4MP1 copolymers. As seen in Figure 5b,c and Figure 6a,b, the saturation times were 5 and 7 s at 145 and 135 °C, respectively, for the C4 copolymer and 14 and 18 s for the 4MP1 copolymer at the corresponding temperatures. Another feature that distinguished the C4 copolymer was a characteristic initial overshoot in the peel curves that significantly exceeded the intrinsic force fluctuations during peeling (Figure 5). The overshoot was not as prominent in the peel curves of the C6 and 4MP1 copolymers at short sealing times; however, it appeared with gradually increasing prominence as the seal time approached the saturation time. Despite the differences in the time behavior, the saturation values of peel strength were practically the same for all copolymers.

The isochronal melt adhesion strength is plotted in Figure 7 for a contact time of 9 s with the functionality

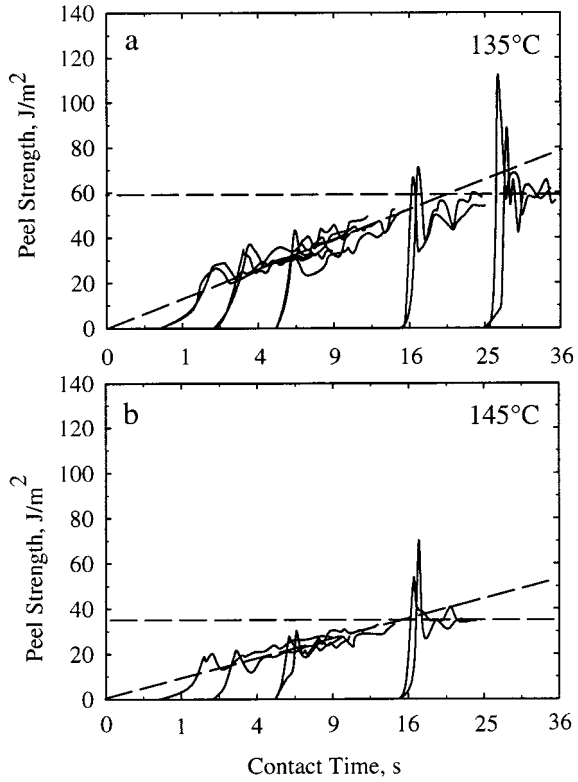

Figure 6. Peel curves of 4MP1 copolymer at different melt temperatures obtained with a peel rate of 500 mm min^{-1} for sealing times of 0.5, 2, and 5 s plotted as a function of total contact time t. The time axis is linear with $t^{1/2}$.

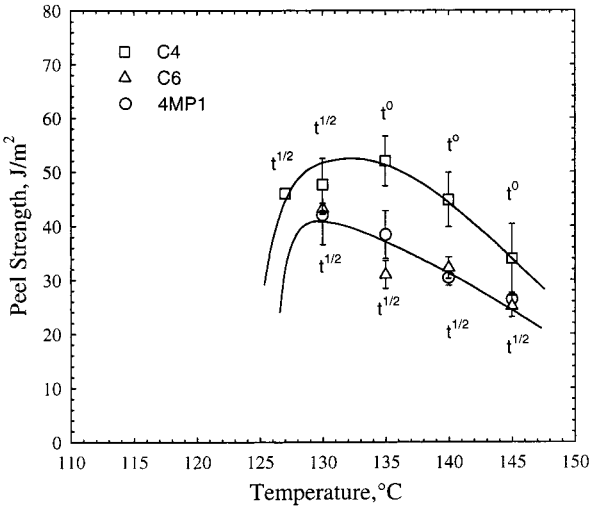

Figure 7. Temperature dependence of the 9 s isochronal peel strength for heterogeneous polyethylene copolymers.

of the time dependence indicated. The C4 copolymer reached saturation faster than other copolymers, and the data at temperatures higher than 130 °C showed the maximum strength. The peel strength for the 4MP1 and C6 copolymers was still increasing at the 9 s contact time, which resulted in the lower values compared to that for C4.

Convergence to the same maximum strength for all copolymers was explored further by peeling at 50 mm/min, an order of magnitude lower rate. In this case, peeling began after contact times of 16−20 s, times that were at or above the saturation time in the higher rate experiments. The fact that all the peel curves in Figure 8 showed constant strength indicated that the saturation time was not dependent on the peel rate. At both temperatures, the curves for the C4 and 4MP1 copolymers overlapped within the range of experimental scatter as expected.

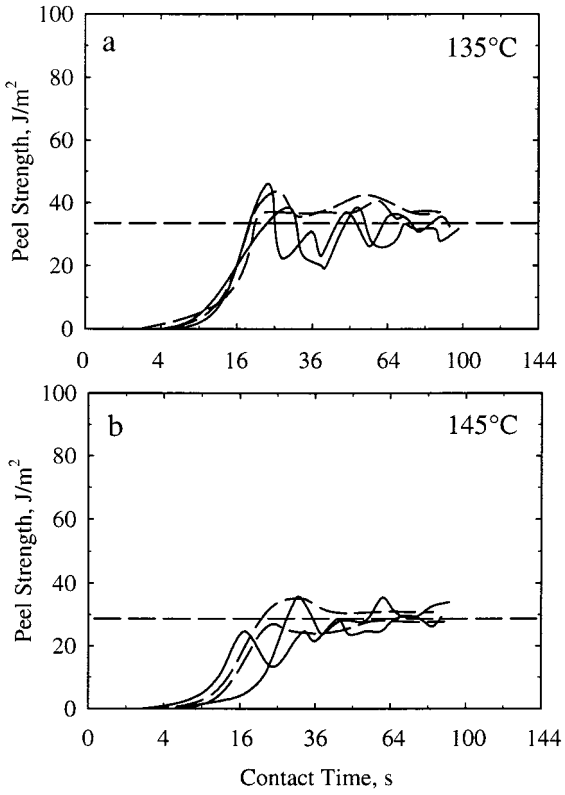

Figure 8. Peel curves of C4 (dashed lines) and 4MP1 (solid lines) at different melt temperatures obtained with a peel rate of 50 mm min^{-1} plotted as a function of total contact time t. The time axis is linear with $t^{1/2}$.

The peel rate did affect the magnitude of the maximum strength, which decreased from 50 to 60 to 30−35 J/m^2 at 135 °C and from 35 to 40 to 28−33 J/m^2 at 145 °C. Rate sensitivity is usual for the peel test due to the complex viscoelastic nature of the processes of deformation and fracture in the damage zone ahead of the running crack. Indeed, the dependence of peel strength on peel rate can be a measure of viscous properties of the material. The rate dependencies of self-adherent un-cross-linked elastomers follow time−temperature superposition with shift factors obeying the Williams−Landel−Ferry relationship.[1,3] A similar situation can be expected for adhesion in the melt if the stress in the damage zone is caused by the viscoelastic response of an extensional melt flow ahead of the peel crack tip. It can be imagined that the pattern of melt flow resembles craze formation and rupture under creep. By analogy, a dilatational strain field ahead of the crack tip causes cavitation and subsequent elongation of the material between the growing cavities as it is drawn into filaments. In this case, the peel strength would be determined by the work to elongate the melt filaments to the breaking strain and could be correlated with the melt strength measured in an appropriate rheological experiment.[27−29]

However, the observed decrease of 20−40% in peel strength upon decreasing the peel rate by an order of magnitude is too small to ascribe the peel strength entirely to viscous dissipation. This indicates that the range of strain rates at the crack tip puts the melt close to the region of the rubbery plateau, where the elastic

component in the viscoelastic response dominates, and stress in the extensional flow is determined mainly by deformation of the entanglement network. This can be confirmed by reference to melt strength experiments for polyethylenes of similar molecular composition.[29] These data showed that both the breaking force and the stretching ratio saturated at strain rates of 10^2 s^{-1} and above. This result is also consistent with a rough estimation of the strain rate $\dot{\gamma}$ from the peel rate v by the relationship[1] $\dot{\gamma} = v/h$, where h is the molten film thickness, which gives a value of 160 s^{-1}. It follows that qualitatively the value of the maximum peel strength at a strain rate higher than the temperature-dependent relaxation rate should be determined by the plateau modulus, which is practically the same for all linear polyethylenes. Because the copolymers had nearly the same average molecular weight (Table 1), all of them achieved the rubbery plateau region at the same strain rate, and the maximum melt adhesion strength was the same at each temperature.

Origin of the Time Dependence. Association of peel strength with the elastomeric response in the rubbery plateau makes it possible to interpret the time dependence in the traditional way as the rate of development of new interfacial entanglements by interdiffusion of surface chains. An abundant literature addresses mechanisms of interdiffusion.[1−4] Although variations in the theory exist, there is general agreement that the time dependence of the interfacial strength reflects the rate of interdigitation of so-called minor chains, i.e., the parts of the original chains that have escaped from their original tubes. The observed $t^{1/2}$ dependence of the peel strength is typical and is commonly ascribed to normal interdigitation of chains with randomly distributed chain ends.[1] The time dependence should saturate at the maximum (cohesive) strength when the chain completely escapes from the original tube and all the surface chain ends reach the interface. This corresponds to the time that is needed for the entire chain to diffuse the distance of approximately a coil dimension. Moreover, a recent study showed that the maximum interfacial strength was achieved even if the interpenetration depth was less than the coil dimension.[30]

However, a serious problem develops when the saturation time in peel strength (t_s), 14−18 s for the 4MP1 and C6 copolymers at 135−145 °C, is compared with the surface chain interdigitation time (τ_i). The latter can easily be estimated from the diffusion coefficient D as $\tau_i = R_g^2/4D$. Here, R_g is the radius of gyration of the polymer coil, which is calculated for polyethylene[31] as $R_g^2 = 2Nb^2$ by using the degree of polymerization $N = M/M_0$, $M_0 = 28$ g mol^{-1}, and the length of the carbon bond $b = 0.154$ nm. The diffusion coefficient of polyethylene is well-known from numerous measurements by various techniques, which are summarized in a previous publication.[19] Because the molecular weight dependence of D conforms well with the prediction from reptation theory, $D \propto M^{-2}$, the diffusion coefficient of polyethylenes is conveniently presented in terms of a prefactor $D^* = DM^2$ that is described by an Arrhenius dependence with an activation energy of 28 kJ mol^{-1}. Reviewed in terms of the prefactor, and reduced to a reference temperature of 175 °C, the values for the diffusion coefficient obtained by various techniques exhibit remarkably good agreement except for a systematic difference by a factor of about 2 between linear and short-chain branched polyethylenes. The value of D^*(175 °C) = 0.33 cm^2 g^2 $s^{-1}mol^{-1}$ is reported for a copolymer with almost the same chemical composition and molecular weight distribution as the copolymers under investigation.[19] Reduced to 145 °C, this gives D^*(145 °C) = 0.19 cm^2 g^2 $s^{-1}mol^{-1}$, which is taken for further evaluation.

For an average molecular weight chain of 120 kg mol^{-1}, which is 2 orders of magnitude higher than the entanglement molecular weight for polyethylene,[32] $M_e \cong 1.4$ kg mol^{-1}, the interdigitation time is $\tau_i \cong 4 \times 10^{-2}$ s at 145 °C. This is about 400 times less than the time $t_s \cong 14$ s to reach the maximum peel strength at this temperature. Accordingly, the interpenetration depth, calculated as $l_s = \sqrt{4Dt_s}$, i.e., a distance that the polyethylene chain has to diffuse before the interface achieves the cohesive strength, is 280 nm for the 4MP1 and C6 copolymers, which is 20 times longer than the radius of gyration of the polyethylene coil (14 nm). Even for the C4 copolymer, which achieved saturation in the peel strength more rapidly (5 s at 145 °C), this depth is estimated to be 170 nm, which is still an order of magnitude larger than the size of the polyethylene coil. Estimates of the interpenetration depth at a lower temperature (135 °C) resulted in the same numbers, suggesting that the interpenetration depth is a characteristic of the film, and therefore the increase in saturation time simply reflects the decrease in diffusion coefficient.

One possible explanation for the discrepancy between experimental data and predictions is the choice of the weight-average fraction as the critical molecular weight fraction. An alternative approach would be to ascribe development of adhesion to extremely slow diffusion of ultrahigh molecular weight chains ($\sim 10^3$ kg mol^{-1}) that are present as a minor fraction in the tail of the molecular weight distribution. Such an interpretation was proposed in a previous study of self-adhesion in deuterated polybutadiene where a similar discrepancy was observed.[21] However, it seems unlikely that chains of the weight-average fraction, which compose most of the material and are long enough to develop a hundred entanglements, do not contribute to the adhesion strength. Furthermore, this explanation cannot account for the difference by a factor of 3 in the saturation times of C4 and the other copolymers when all have similar molecular weight distribution and the same value of the maximum peel strength. Moreover, if a minor fraction determines the toughness of the entanglement network, the melt strength of polyethylenes with very different polydispersity would not correlate with the average molecular weight.[28] It becomes evident that the traditional interdigitation model does not work for the polymers in this study.

Surface Layer. The heterogeneous molecular structure of the polyethylenes under investigation suggests another interpretation of the saturation time scale and large interpenetration depth. The discrepancy in the interdigitation time could indicate the existence of a surface layer that the bulk chains must diffuse through in order to achieve the maximum adhesion strength. This implies that the surface layer is inert in terms of adhesion; i.e., when two surface layers are brought together in the melt, they are not capable of developing good tack. This is possible if the surface layer consists of low molecular weight, highly branched chains.

Segregation of low molecular weight chains to the surface is well-known and exists even for linear ho-

mopolymers.[2,33] Qualitatively, the driving force for segregation is of both entropic and enthalpic origin. The entropic reason for segregation is halving in the conformational freedom of polymer chains on the surface compared to chains in the bulk. Thus, locating chains on the surface is not profitable in terms of thermodynamic free energy. However, the shorter the chain, the less freedom it has and, hence, the less entropy is lost if this chain is located on the surface. The enthalpic reason for segregation is the decrease in surface energy due to the interaction of chain ends. Shorter chains have a higher concentration of chain ends per unit volume. The enthalpic advantage for surface segregation can be considerably enhanced by changing the chain topology to increase the concentration of chain ends, for example by mixing linear chains with stars or brushes of the same backbone structure.[33−35]

Introduction of short-chain branches by copolymerization of ethylene with an α-olefin increases the effective number of chain ends proportionally to the comonomer content. Enhancement of the interaction can result in immiscibility of linear polyethylene with short chain branched polyethylenes of high enough copolymer content in the melt.[24,25] It is well-known that linear low-density polyethylenes produced by conventional Ziegler−Natta catalysts are characterized by a wide molecular weight distribution and considerable nonuniformity in comonomer distribution. The broad distribution in comonomer content is seen in the TREF curves in Figure 2; furthermore, the chains with highest concentration of short chain branches are also those in the low molecular weight tail of the molecular weight distribution.[18] Consequently, short chains that are driven to the surface by the entropic contribution to the chemical potential also have an enthalpic advantage in moving to the surface. In very thin films prepared from model blends of polyolefins, dramatic surface enrichment by a highly branched component is well established.[36,37] Just recently, demonstration of an amorphous surface layer on conventional blown polyethylene film was achieved by atomic force microscopy.[38]

The longer saturation time for the 4MP1 and C6 copolymers can now be understood. Appearance of two peaks in the TREF curves of 4MP1 and C6 copolymers suggests a "blendlike" composition, whereas the C4 copolymer is much less heterogeneous in terms of comonomer distribution. Because the thermodynamic advantage for surface segregation correlates with the excess comonomer content of low molecular weight chains, the surface layer should be thicker for 4MP1 and C6 than for C4. Accordingly, the interpenetration depth, which can be considered as the doubled thickness of the layer, was estimated from the diffusion coefficient and saturation times as 280 and 170 nm for 4MP1 and C4 copolymers, respectively. However, these numbers should be considered as estimates only; differences in the interaction parameter χ between segregated fractions and regular bulk chains might affect the diffusion coefficient.[39,40]

Upon the joining of two surface layers in the melt, fast interdiffusion of low molecular weight chains rapidly resolves the weldline. However, low molecular weight fractions cannot create good adhesion. They disentangle as easily as they interdiffuse; the same molecular reptation dynamics underlie both processes. However, as soon as the surfaces are brought together, they become part of the bulk and the thermodynamic advantage for segregation ceases. The joined surface layers become merely a composition fluctuation in the bulk. Homogenization by mutual interdiffusion brings long chains to the interface. The kinetics of interdigitation of bulk chains at the interface, which plays a key role in the traditional interpretation of adhesion, is not important in the present consideration because interdigitation is much faster than homogenization. Therefore, the peel strength during the process of interdiffusion should be proportional to the amount of bulk material that reaches the interface, which explains the $t^{1/2}$ dependence. The peel strength saturates when the segregated layers completely resolve, and the molecular composition at the interface becomes the same as in the bulk.

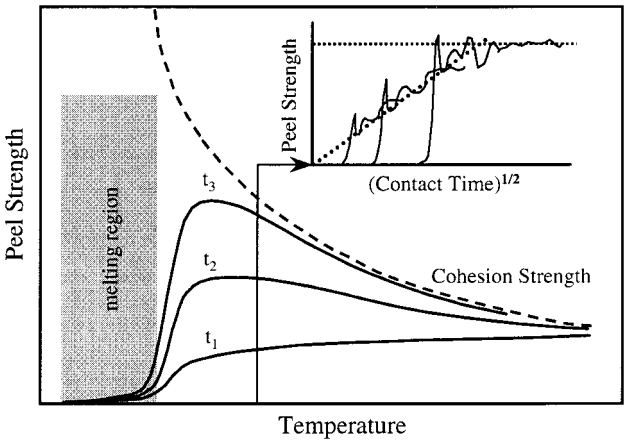

Figure 9. Schematic model of the time−temperature dependence of adhesion in the melt.

The schematic representation of the time and temperature dependence of the interfacial adhesive strength in Figure 9 is based on the proposed sealing mechanism. The isochronal curves labeled t_1-t_3 represent the adhesive strength as a function of temperature at different contact times. The shapes of these curves reflect competition between the increasing rate of interdiffusion with temperature, which results in a faster approach to the maximum (cohesive) strength, and the decrease the maximum strength with temperature. Measurable peel strength did not develop in the melting region (shaded zone in Figure 9). This was because the low molecular weight amorphous surface layer was incapable of developing good adhesion, and the long chains in the bulk were anchored in incompletely melted crystallites which prevented them from diffusing freely to the interface. A previous study showed that the time required for heat sealing of linear low-density polyethylene was 3 orders of magnitude higher in the melting range than in the melt.[41] However, the maximum strength in the melting range, when achieved, is obviously much greater than in the melt because of partial crystallization at the interface.

Crystallization at the interface cannot be completely disregarded even above the melting region. The extensional flow ahead of the peel crack may cause strain-induced formation of extended chain crystals.[42−44] These crystals melt at higher temperatures than lamellar crystals, reportedly at 145−160 °C for polyethylene.[42,45] Formation of strain-induced crystals depends on the degree of chain orientation, which is a function of the ratio between the rate of elongation and the relaxation time. Formation of extended chain crystals is also inhibited by short-chain branches which are not allowed

in the polyethylene crystal. Obviously, low molecular weight chains in the surface layer that have a short relaxation time and high comonomer content are not candidates for strain-induced crystallization. Crystallization would be favored by high strain rates and at longer contact times as more long chains diffuse to the interface. Strain crystallization would also be favored by a more homogeneous comonomer content. These conditions correlate with the appearance of the initial overshoot in the peel curves in Figures 4 and 5. The strain rate at initiation is always higher than the rate during steady-state propagation in the peel test.[46] The overshoot was higher for the C4 copolymer than the 4MP1 and C6 copolymers; the overshoot in the latter materials occurred only as saturation was approached. Considering also the absence of an overshoot at the lower peel rate (50 mm s^{-1}), the association with strain-induced crystallization seems reasonable.

Conclusions

This study concerned the development of self-adhesion above the melting temperature in a series of short-chain branched polyethylenes. The materials were similar in molecular weight distribution but differed in the chemical structure of the comonomer and the heterogeneity of the comonomer content. It was found that the peel strength increased with the contact time in accordance with the conventional $t^{1/2}$ dependence until saturation at the maximum strength. The time to achieve the maximum strength, on the order of seconds, was shorter for the material with more homogeneous copolymer composition; however, the maximum strength was the same for all of the materials at each temperature. Furthermore, the saturation time in all cases was 2 orders of magnitude longer than the time for complete interdigitation of the surface chains. This was ascribed to the presence of a surface layer of about 100 nm that the bulk chains needed to diffuse through in order to develop cohesive strength. The layer was thought to originate from surface segregation of the lower molecular weight, higher branch content fraction of the material. In this respect, the occurrence of the surface layer was inherent for a polymer with heterogeneous molecular composition.

The hypothesis of the surface layer in heterogeneous copolymers can be tested by comparing the melt adhesion of metallocene copolymers which have homogeneous comonomer content distribution and narrower molecular weight distribution. The postulated surface layer should not exist in these materials. Accordingly, the melt adhesion should reach the maximum strength instantaneously on the experimental time scale. Furthermore, the surface layer can be experimentally modeled by blending metallocene copolymers of different comonomer content in either miscible or immiscible compositions. These issues are addressed in a subsequent contribution.

Acknowledgment. This research was generously supported by BP Amoco Chemicals.

References and Notes

(1) Wool, R. P. *Polymer Interfaces*; Hanser: Munich, 1995.
(2) Jones, R. A.; Richards, R. W. *Polymers at Surfaces and Interfaces*; Cambridge University Press: New York, 1999.
(3) Brown, H. R. *Annu. Rev. Mater. Sci.* **1991**, *21*, 463−489.
(4) Kausch, H. H.; Tirrell, M. *Annu. Rev. Mater. Sci.* **1989**, *19*, 341−377.
(5) Ligoure, C. *Macromolecules* **1996**, *29*, 5459−5468.
(6) De Gennes, P. G. *Langmuir* **1996**, *12*, 4497−4500.
(7) Gent, A. N.; Kim, E.-G.; Ye, P. *J. Polym. Sci., Part B: Polym. Phys.* **1997**, *35*, 615−622.
(8) Brochard-Wyart, F.; de Gennes, P. G.; Leger, L.; Marciano, Y.; Raphael, E. *J. Phys. Chem.* **1994**, *98*, 9405−9410.
(9) Bensason, S.; Minick, J.; Moet, A.; Chum, S.; Hiltner, A.; Baer, E. *J. Polym. Sci., Part B: Polym. Phys.* **1996**, *34*, 1301−1315.
(10) Chen, H. Y.; Stepanov, E. V.; Chum, S. P.; Hiltner, A.; Baer, E. *Macromolecules* **2000**, *33*, 8870−8877.
(11) Doi, M.; Edwards, S. F. *The Theory of Polymer Dynamics*; Oxford University Press: New York, 1986.
(12) *Theoretical and Mathematical Models in Polymer Research*; Grosberg, A., Ed.; Academic: Boston, 1998.
(13) Cramm, R. H. *Tappi J.* **1989**, *72* (3), 185−189.
(14) Van der Sanden, D. G. F.; Halle, R. W. *Tappi J.* **1992**, *75* (2), 99−103.
(15) Halle, R. W.; Davis, D. S. *Tappi J.* **1995**, *78* (2), 200−206.
(16) Shih, H.-H.; Wong, C.-M.; Wang, Y.-C.; Huang, C.-J.; Wu, C.-C. *J. Appl. Polym. Sci.* **1999**, *73*, 1769−1773.
(17) Williams, J. G. *Fracture Mechanics of Polymers*; Ellis Horwood: Chichester, 1984.
(18) Wild, L. *Adv. Polym. Sci.* **1990**, *98*, 1−198.
(19) Schuman, T.; Stepanov, E. V.; Nazarenko, S.; Capaccio, G.; Hiltner, A.; Baer, E. *Macromolecules* **1998**, *31*, 4551−4561.
(20) Schuman, T.; Nazarenko, S.; Stepanov, E. V.; Magonov, S. N.; Hiltner, A.; Baer, E. *Polymer* **1999**, *40*, 7373−7385.
(21) Roland, C. M.; Bohm, G. G. A. *Macromolecules* **1985**, *18*, 1310−1314.
(22) Von Seggern, J.; Klotz, S.; Cantow, H.-J. *Macromolecules* **1991**, *24*, 3300−3303.
(23) Pearson, D. S.; Fetters, L. J.; Graessley, W. W.; Ver Strate, G.; Von Meerval, E. *Macromolecules* **1994**, *27*, 711−719.
(24) Morgan, R. L.; Hill, M. J.; Barham, P. J.; Frye, C. J. *Polymer* **1997**, *38*, 1903−1909.
(25) Crist, B.; Hill, M. J. *J. Polym. Sci., Part B: Polym. Phys.* **1997**, *35*, 2329−2353.
(26) Bonner, J. G.; Frye, C. J.; Capaccio, G. *Polymer* **1993**, *34*, 3532−3534.
(27) Micic, P.; Bhattacharya, S. N.; Field, G. *Int. Polym. Process.* **1997**, *XII*, 110−115.
(28) Ghijsels, A.; Ente, J. J. S. M.; Raadsen, J. *Int. Polym. Process.* **1990**, *V*, 284−286.
(29) La Mantia, F. P.; Acierno, D. *Polym. Eng. Sci.* **1985**, *25*, 279−283.
(30) Schnell, R.; Stamm, M.; Creton, C. *Macromolecules* **1998**, *31*, 2284−2292.
(31) La Mantia, F. P.; Acierno, D. *Polym. Eng. Sci.* **1985**, *25*, 279−283.
(32) Wu, S. *J. Polym. Sci., Part B: Polym. Phys.* **1989**, *27*, 723−741.
(33) Wu, D. T.; Fredrickson, G. H. *Macromolecules* **1996**, *29*, 7919−7930.
(34) Schaub, T. F.; Kellog, G. J.; Mayes, A. M.; Kulasekere, R.; Ankner, J. F.; Kaiser, H. *Macromolecules* **1996**, *29*, 3982−3990.
(35) Frischknecht, A.; Fredrickson, G. H. *Macromolecules* **1999**, *32*, 6831−6836.
(36) Scheffold, F.; Budkowski, A.; Steiner, U.; Eiser, E.; Klein, J.; Fetters, L. J. *J. Chem. Phys.* **1996**, *104*, 8795−8806.
(37) Brant, P.; Karim, A.; Douglas, J. F.; Bates, F. S. *Macromolecules* **1996**, *29*, 5628−5634.
(38) Magonov, S.; Godovsky, Y. *Am. Lab.* **1999**, *31* (8), 52−58.
(39) Kramer, E. J.; Green, P.; Palmstrom, C. J. *Polymer* **1984**, *25*, 473−480.
(40) Brochard, F.; Jouffroy, J.; Levinson, P. *Macromolecules* **1983**, *16*, 1638−1641.
(41) Mueller, C.; Capaccio, G.; Hiltner, A.; Baer, E. *J. Appl. Polym. Sci.* **1998**, *70*, 2021−2030.
(42) Wunderlich, B. *Macromolecular Physics*; Academic: Boston, 1980; Vol. 3.
(43) Mandelkern, L. *Comprehensive Polymer Science*; Pergamon: Oxford, 1989; Vol. 2.
(44) Mackley, M. R.; Keller, A. *Philos. Trans. A* **1975**, 29−66.
(45) Chvalun, S. N.; Bessonova, N. L.; Konstantinopol'skaya, M. B.; Zubov, Yu. A.; Bakeev, N. F. *Dokl. Phys. Chem.* **1987**, *294*, 614−617.
(46) Kendall, K. *Int. J. Fract.* **1975**, *11*, 3−12.

MA000583X